Jurnal Teknologi

Full paper

# A Study on Estimation of Propulsive Power for Wing in Ground Effect (WIG) Craft to Take-off

Priyanto, A.[a*], Maimun, A.[a], Noverdo, S.[a], Saeed, J.[a], Faizal, A.[a], Waqiyuddin, M.[a]

[a]*Department of Marine Technology, Faculty of Mechanical Engineering, Universiti Teknologi Malaysia, 81310 UTM Johor Bahru, Johor, Malaysia*

*Corresponding author: agoes@fkm.utm.my

**Article history**

Received :12 January 2012
Received in revised form :18 June 2012
Accepted :13 August 2012

**Graphical abstract**

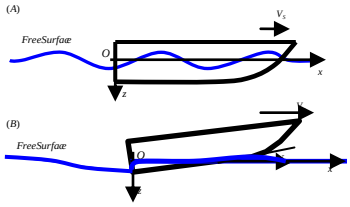


**Abstract**

This paper estimated the propulsive power required for Wing in Ground effect (WIG) craft to take-off. The hull form design of the WIG craft incorporates a stepped planing triple hull, since the planing hull is well known to give result and assist in lifting off the water surface effect. In order to determine the power required for WIG craft to take-off, the craft prototype was built into 1 to 6 model scale. In numerical calculation, the required thrust motor of model to take-off was calculated by summation of water drag; aerodynamic drag and the weight of model. The water drag was estimated by Savitsky's method, and the aerodynamic drag by a MATLAB programming based on Vortex Lattice Method (VLM). In the experiments, the relationship propeller RPM against thrust motor was obtained from the calibration tests. At the flight tests of the model, the propeller RPM of the model was measured to determine the total thrust motor and the propulsive power required to take-off by using the Froude's Momentum Theory. The required propulsive power for craft scaled model was found to give the total thrusts of 33.85 N, and the effective power estimates required for WIG model to take-off per propeller was 128Watt at the design speed. It was also observed during most of the flight tests, the craft is attempting to enter into ground surface effect at design speed.

*Keywords:* WIG craft; propulsive power; water drag; aerodynamic drag; thrust motor

**Abstrak**

Kertas kerja ini mengira jumlah kuasa bagi bot Wing in Ground effect (WIG) untuk terbang. Perekabentuk bot WIG menggunakan badan bot planing, yang terkenal untuk membantu dan mengangkat badan bot ke atas permukaan air. Dalam mendapatkan kuasa bagi bot WIG untuk terbang, model bot dibina dalam skala 1 berbanding 6. Pengiraan kuasa bagi model WIG adalah pengiraan jumlah rintangan model pada setiap halaju, terhadap tambahan rintangan udara, rintangan air dengan jisim model. Kaedah yang digunakan dalam pengiraan jumlah rintangan model adalah dua kaedah iaitu kaedah berangka dan eksperimen. Dari kaedah berangka, rintangan air telah dikira menggunakan simulasi Savitsky, dan rintangan udara telah dikira menggunakan simulasi MATLAB berasaskan kaedah Vortex Lattice Method (VLM). Dari kaedah eksperimen, ujian kalibrasi dilakukan terlebih dahulu untuk mendapatkan hubungan antara RPM melawan daya dorong. Kemudian ujian terbang dilakukan untuk mendapatkan RPM untuk setiap halaju model sebelum terbang. Nilai RPM daripada ujian ini digunakan untuk mendapatkan jumlah daya dorong daripada ujian kalibrasi dan jumlah kuasa didapatkan dengan menggunakan persamaan hukum Froude's Momentum. Keputusan jumlah daya dorong bagi model diperlukan untuk terbang daripada dua kaedah adalah 33.85 N, dan jumlah kuasa untuk satu kipas iaitu 128Watt. Daripada pengamatan ujian terbang, model WIG telah terbang dalam Ground Effect (GE) di atas permukaan air.

*Kata kunci*: Bot WIG; jumlah kuasa; rintangan air; rintangan udara; jumlah daya dorong daripada motor



## 1.0 INTRODUCTION

The Wing in Ground (WIG) craft also called ekranoplan or Ground Effect Machine (GEM) is a high speed low altitude flying vehicle that utilizes a favourable ground effect. This effect appears at about one wing chord distance from the ground and results in an enhanced lift-drag ratio. WIG craft is a new marine transport that is developed according to aircraft environment application. Speeds of WIG craft are much higher than those of ships, and operational expenses are much lower than those of airplanes. Besides that, more advantages of most WIG craft vehicles are their amphibious properties. Moreover, WIG craft

can take off and land on any relatively flat surface, such as land, water, snow, and ice. The usage of the ground effect has also been discovered in nature: birds and flying fish spent less energy moving in the vicinity of water surfaces. The most significant contribution to the progress of the WIG concept was made in Russia by the Central Hydrofoil Design Bureau under the guidance of R.E. Alekseev, who developed a number of unique test crafts (the series SM and the famous Caspian Monster KM), as well as the first serial vehicles of Orlyonok and Lun types [1].

The need of increasing the speed and payload of the marine transportation has prompted many research developments on high speed marine vehicles (HSMVs). Planing craft is a HSMV which may generate the lift force by well-designed hull. Numerical modeling of this problem is an important subject in ship design and naval architect. Experiments have shown that the deadrise angle and the well-designed bottom shape of the hull are very important in the planing crafts. The effect of the deadrise angle on hydrodynamic force, impact loading on the hull and high planing efficiency lead to a rational deadrise angle between $10^{\circ} \le \overline{\beta} \le 15^{\circ}$ [2]. Although the low deadrise angle and the chine enhance seakeeping performances but they may instigate other insufficiency problems like more slamming and porpoising (i.e. combined heaving and pitching instability). The form of stern is another aspect that is important in the craft design. The transom stern is a common choice used in planing crafts. A number of advantages of this stern type are weight reduction, manufacturing efficiency and possible resistance decrease in the speed range of craft operation.

Prediction of the water drag of a WIG craft categorized as the high-speed planing hull should be carried out in the first part of the designing process in order to estimate the required power for the propulsor and main engine. From the numerical point of view, resistances study of planing body in calm water experiences have been performed by many researchers in the past two decades, involving steady/unsteady numerical analysis. Lai and Troesch [3] applied a vortex lattice method to the planing body using the slender body theory. Zhao et al. [4] introduced the strip theory for steady planing in calm water. Savander et al. [5] used the boundary value problem for steady planing surfaces. Xie et al. [6] reported the study of the hydrodynamic problem of 3-D planing surface by using the vortex theory and the finite element approach. Hydrodynamic analysis of the planing hull at high Froude number was performed by Wang and Rispin [7] and Cheng and Wellicome [8]. Ghassemi and Ghiasi [2] used nonlinear free surface boundary condition for the submerged lifting and non-lifting bodies using Boundary Element Method (BEM).

Clement and Blount [9] conducted an extensive set of model tests on a systematic series (Series 62 model 4666). Katayama et al. [10] performed the resistance tests on the prismatic planing hulls at various speeds and reported lift, resistance and moment coefficients. Savistky [11] had made a great contribution to the understanding and modeling of planing hull. He developed regression formulas based on prismatic hull form model tests to estimate the hydrodynamic forces.

In order to predict the aerodynamic drag of WIG crafts flying both in and out of the ground effects, many theoretical studies have been carried out, including methods for predicting lift and drag, as well as overall aerodynamic performance, and considerable progress has been made in this direction. For two-dimensional airfoils with or without flaps and airlerons, numerous calculation methods based on potential theory arc now available, refer to Steinbach and Jacob [12]. For three-dimensional wing and wing with end-plate, potential theory methods such as the panel and the vortex lattice methods are developed. The objective of this paper is to continue the development of three-dimensional vortex lattice methods for the aerodynamics analysis of the WIG craft. Numerical results include lift and drag. The required thrust motor of model to take-off was calculated by summation of water drag, aerodynamic drag and the weight of model. Numerical calculation for the water drag of WIG hull used Savitsky's method. In the experiments of the flight tests, the propeller RPM of model was measured and determined, then the total thrust motor was calculated by using the relationship data between RPM and thrust given from the calibration tests. The results of the flight tests and the numerical test were compared.

## 2.0 HULL FORM DESIGN AND DRAG CALCULATION

### 2.1 Hull Form Design

Based on the literature review for the design of hull model there are at least 3 features that are essential to the seaplanes, which the WIG model can adopt. The hull form should be of a deep-V configuration to facilitate the craft in high speed. Next, dead-rise angles should not exceed $24^0$; $15^0$ for moderate waves and any lower would be suitable for flat water [2]. The third consideration would be the incorporation of a stepped hull with the addition of using outrigger double hull as shown in Figure 1. Using an outrigger or double hull configuration greatly increases the stability of the WIG model. A design is then conceptualized on drawing based on these inputs as well as the essential features as shown in Figure 2.

**Figure 1** Outrigger Canoe

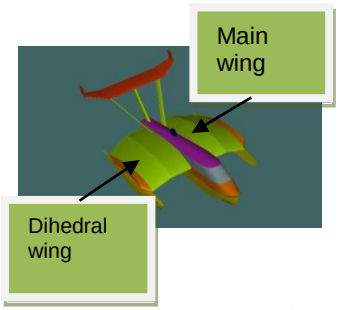


**Figure 2** Outrigger WIG craft

The principle dimensions of the model have been decided as shown in Table. 1 with further input from control part that a certain internal space is required for the control systems.

**Table 1** Principle dimensions of two seater wing-in ground effect craft

| **Main Wing** | Prototype | Model (Scale 1:6) |
|---|---|---|
| Wing section | S-shape (NACA6409) | S-shape (NACA6409) |
| Area | 9.974m$^2$ | 0.277m$^2$ |
| Span | 1.496m | 0.249m |
| Tip chord | 3.996m | 0.666m |
| Root chord | 3.996m | 0.666m |
| Dihedral angle | $0^0$ | $0^0$ |
| **Dihedral Wing** | | |
| Wing section | S-shape (NACA6409) | S-shape (NACA6409) |
| Area | 9.974m$^2$ | 0.277m$^2$ |
| Span | 3.496m | 0.582m |
| Tip chord | 3.996m | 0.666m |
| Root chord | 3.996m | 0.666m |
| Dihedral angle | $13^0$ | $13^0$ |
| **Hull** | | |
| Length over all (LOA) | 7.23m | 1.205m |
| Breadth over all (B) | 4.998m | 0.833m |
| Hull breadth | 0.798m | 0.133m |

### 2.2 Hull Water Drag (Savitsky's Method)

Research has shown that the most basic hull design of WIG craft uses a hull planing and this assists in lifting off the water surface as shown in Figure 3. In October 1964, a comprehensive paper that summarized previous experimental studies on the hydrodynamics of prismatic planing surfaces was presented by Savitsky [11]. He presented a method for application of these results for the design of moving ships.

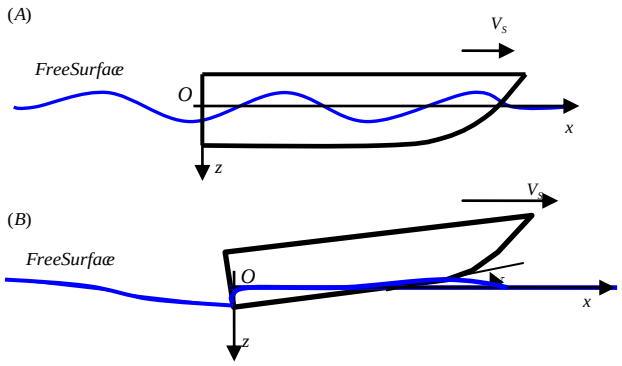


**Figure 3** Basic hull system for planning (B) and non-planing hull (A)

Savitsky's Method was based on the hydrodynamic planing boat power prediction method. WIG hull would trim at certain angle where the fore of the boat will lift out of the water surface and the aft will partly immersed in the water where the lift and the resistance will react on the surface of the hull. The hull is assumed to run in steady state in calm water, i.e. with constant speed $V_S$, draft, and trim angle $\tau$ . The flow velocity component normal to the keel is $U = V_S \sin\tau$ . The principal characteristics in the chine-dry region is illustrated in the section *E-E* (Figure 4). It is shown that the water surface is deformed and piles-up is closed to the hull. At the spray root, i.e. the intersection between the piled-up water line and the hull, a spray-jet is formed. The peak of the hydrodynamic pressure distribution relates to the formation of the jet. In the chine-wet region (section *F-F*), the sideway flow separates at the sharp chine, where the hydrodynamic pressure adjusts to atmospheric pressure. The hydrodynamic pressure of the spray is proportional to the geometrical configuration of the hull such as the deadrise, the trim, and chine wet/dry regions and operation conditions like the speed and the water wave.

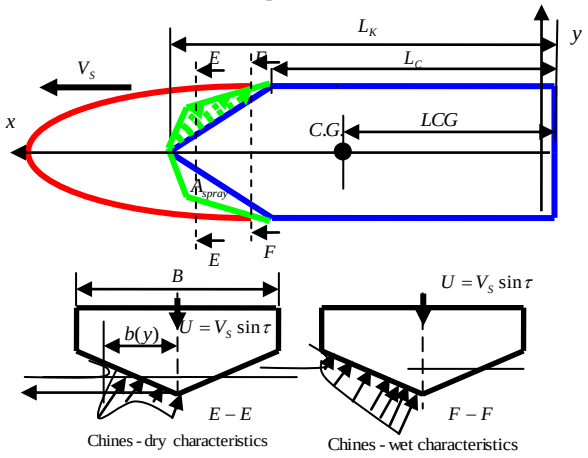


**Figure 4** Spray surface and transverse pressure distribution

Centre of pressure for a hull planing surface is given by Ghassemi and Ghiasi [2] as:

$$C_p = \frac{L_{CP}}{L_M} - 0.75 - \left( \frac{1}{5.21 + C_v^2 / \lambda^2 + 2.39} \right) \quad (1)$$

Where:

$$\lambda = \frac{(L_K + L_C)}{2B}$$

$$L_K = L_M + \frac{b \tan\beta}{2\pi \tan\tau} \qquad L_C = L_M - \frac{b \tan\beta}{2\pi \tan\tau}$$

$L_K$ is keel wetted length, $L_C$ is chine wetted length, $B$ is hull breadth, $\beta$ and $\tau$ are deadrise and trim angle, respectively.

The centre of pressure can be calculated as;

$$L_{CP} = C_P \lambda\beta = C_P L_M \quad (2)$$

For speed coefficient or "Breadth – Froude Number" is given by the following equation;

$$C_v = \frac{V_s}{\sqrt{gb}} \quad (3)$$

The total hydrodynamic drag of a planing surface is composed of pressure drag developed by pressure acting normal to the inclined bottom and viscous drag acting tangential to the bottom in both of pressure area and spray area:

$$D = \Delta \tan\tau + \frac{D_f}{\cos\tau} \quad (4)$$

$$D_f = \frac{C_f \rho V_1^2 \left(\lambda b^2\right)}{2\cos\beta^4} \quad (5)$$

Where $C_f$ is applied according to International Towing Tank Conference (ITTC, 1957) [13] friction line, and is given by the following:

$$C_f = \frac{0.075}{\left(LogR_n - 2\right)^2} \quad (6)$$

### 2.3 Wing aerodynamic drag (Vortex Lattice Method)

Drag force of the wing is the total force caused by air cushion pressure on the main wing, while drag force of fuselage is the total forces that acts on the hull above water. Drag at the tail of this model was assumed negligible. There are many methods that can be used to model a wing motion in proximity to the ground. Many methods at present are used; i.e. simple channel models, analytical asymptotic approaches, potential panel methods, and modern finite volume methods. Most of critical design problems can be solved by use of panel methods. The vortex lattice method

(VLM) in this paper were used to represents the best trade-off between accuracy and required computational resources for a certain class of problems. Motion of a WIG craft before it take-off can be divided into two regimes, they are:

(1) The transitional mode, when the Froude number $F_n = V_\infty / \sqrt{gD^{1/3}} < 3$, where $V\infty$ is the speed and $D$ is the displacement of a vehicle;
(2) The planing mode with aerodynamic unloading, when $F_n > 3$.

Present numerical study was carried out by a model of rectangular wing for validation purposes and some compound dihedral wings design with NACA6409 airfoil section. The principle dimensions of the wings (Refer Figure 5) are shown in Table 1. These simulations were prepared with respect to different angles of attack (AOA) and ground clearance (*h/c*), aspect ratio and velocity of airflow 25.5 m/s. Ground level (*h*) is defined as the distance between the trailing edge of wings center and ground surface.

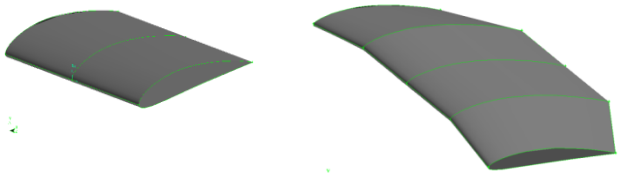

(a) Rectangular wing (b) Compound wing

**Figure 5** Wing Shape of WIG Craft

For the traditional representation of flat wing, the vortex lattice is located in plane parallel to free stream. The velocity induced by a straight vortex element can be calculated by Biot-Savart law which takes the form as (Lai and Troesch [3]):

$$U = \frac{1}{4\pi}\Gamma_n \frac{dl.r}{[r]^3} \tag{7}$$

Equation (5) was then integrated to give the induced velocity for a vortex segment of arbitrary length.

$$U = \frac{1}{4\pi}\Gamma_n \frac{r_1 r_2}{[r_1.r_2]^2}\left[r_0\left(\frac{r_1}{r_2} - \frac{r_2}{r_1}\right)\right] \tag{8}$$

From equations (4) and (6) the downwash, sidewash and backwash velocities can be expressed as :

$$U_{u,v,w} = \frac{1}{4\pi}\Gamma_n F_{u,v,w}(x, y, z, s, \psi, \phi) \tag{9}$$

The coefficient along an elemental length of chordwise and coefficient divided by free stream dynamic pressure can be expressed to implement equation (9) in *Kutta-Joukowski* theorem. This gives the following Lift coefficient equation :

$$C_L = 2\sum_n^{N/2}\left(\frac{2}{S}\Gamma_n c_c U_{u,v,w}\right) + \sum_n^{N/2}\left(\frac{2}{S}\Gamma_n 2b\right)\left[(1-U_{u,v,w}) + (U_{u,v,w})\tan\psi\right]\cos\phi \tag{10}$$

The frictional drag can be deduced from the induced drag;

$$C_D = (1-\varphi)\frac{C_L^2 S}{\pi b^2} \tag{11}$$

Where;

$$\varphi = \frac{1.66\dfrac{2h}{c}}{1+1.66\dfrac{2h}{c}} \tag{12}$$

## 2.4 Propulsive Power Estimation

The components of thrust for the model consist of the weight of the model, the aerodynamic drag and the water drag value. Figures 6, 7 and 8 show the results of the hull water drag for main and double outrigger hulls, the aerodynamic drag and total WIG model drag. The design break down weight of the model represents the servo components, the motor and construction methods as shown in Table 2., which was completed with the total weight of 7.75 N.

**Tabel 2** Weight breakdown of WIG model

| Components | Mass in kg | % total mass |
|---|---|---|
| Structural (hull, tail, wing) | 0.54 | 68 |
| Propulsion (2 ducted propellers and motor) | 0.10 | 12 |
| Control and servo components | 0.15 | 20 |
| Total | 0.79 | 100 |

From Table 2 and Figure 8, the required power for craft prototype was calculated at the design air speed of 10.28m/s to give the total thrusts of 33.85 N. Since the configuration of the model have 2 propellers, it may be assumed that the total thrust is divided by two with same type of motor, thus each of them is 17 N. Therefore the effective power estimates required for WIG model to take-off per propeller based on Froude's momentum theory (Houghton and Carpenter, [14]) will be 128Watt at the design speed.

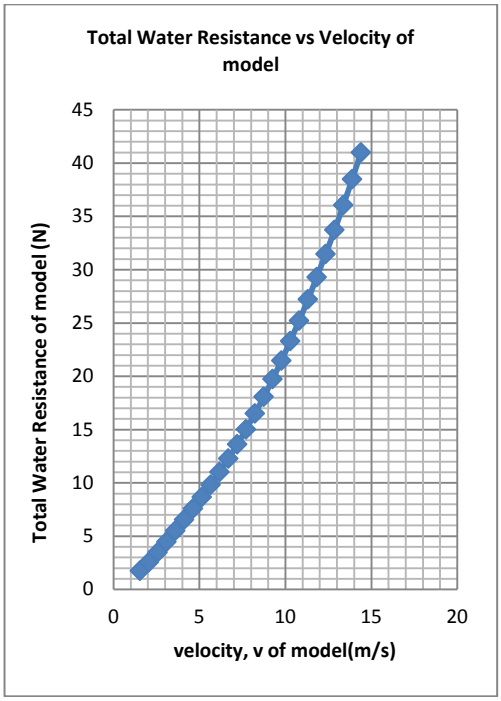


**Figure 6** Hull water drag (resistance)

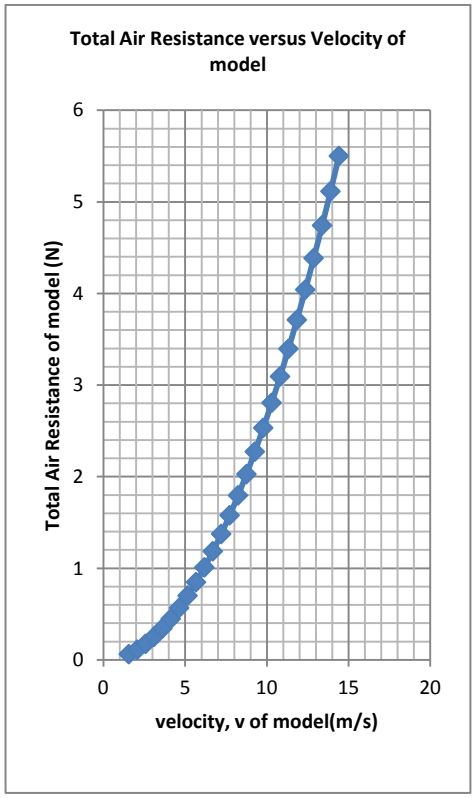


**Figure 7** Aerodynamic drag (resistance)

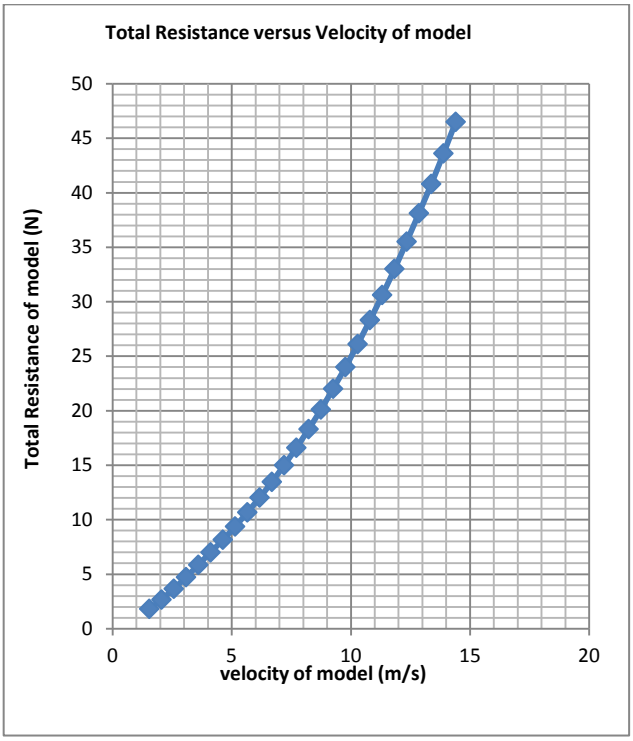


**Figure 8** Total drag (resistance)

The power required is in the lower range and it is found that the electric motor is feasible rather than the usual internal combustion engine. Due to cost, weight and operability considerations in the model experiments, the MAXX ducted brushless motor as shown in Figure 9 was then deployed. The ducted brushless motor, based on its specification, can supply a maximum thrust of 2.5kg or 24.5 N.

**Figure 9** MAXX ducted brushless motor

## 3.0 MODEL EXPERIMENTS

Free running test is divided into two parts, the telemetry data records and calibration rig. Telemetry data system will provide results directly, where the data is the propeller rate (rpm) versus ship's speed. Calibration test rig was conducted to determine the amount of thrust for each rpm of the DC motor. Then the data that is obtained from the telemetry system can be roughly converted from the calibration rig (refer to Figure 10 to 12).

A side view of the craft was taken to measure the cruising height. A simple piece of rope (attached to the bottom of the craft) was taken and divided into separate segments. Each segment represents 1 cm. From Vortex Lattice Method (VLM) and Fluent

(CFD), it was observed that the maximum theoretical height was 5cm above ground.

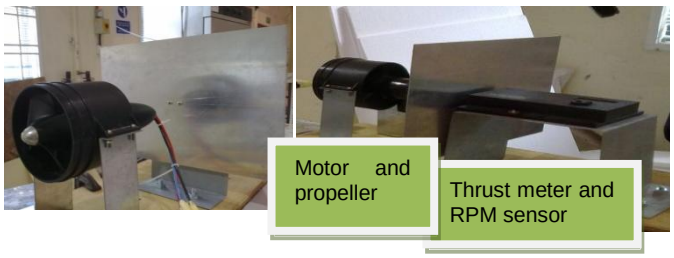


**Figure 1** The propeller and thrust motor calibration rig

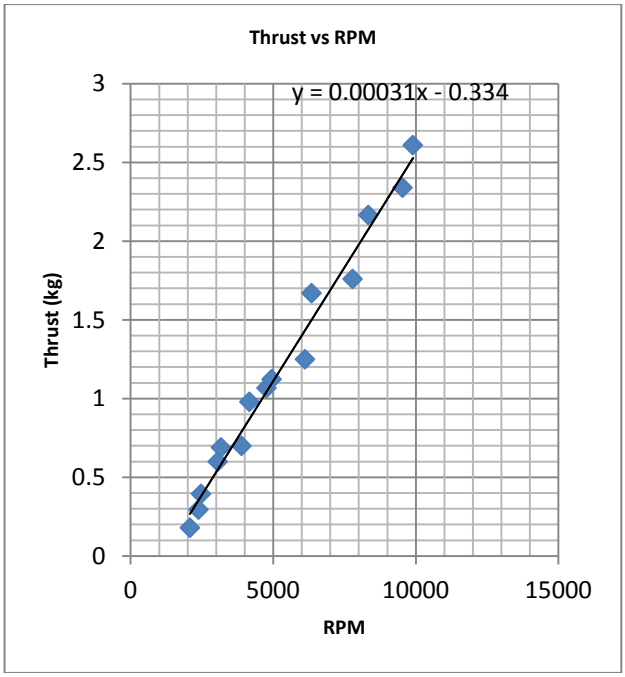


**Figure 11** The propeller RPM and thrust motor measurement

During flight test, there are some installed sensors, namely; the pitot tube, temperature sensor, and T-junctions, and telemetry system. The pitot tube was placed at the forward hull in order to obtain the precise craft's speed measurement. Pitot tube is used to measure the speed of the WIG model as it moves at the water surface or over the water surface (flight test). It also serves as a measure of elevation by detecting the total difference in air pressure when the WIG model is flying. The temperature sensor is used to detect the temperature of the battery storage box. The temperature of the heat generated by the battery detected by the (temperature sensor) is entered into the data recorder before it is transmitted by telemetry system transmitter. The data can then be viewed on the PC screen dashboard. The temperature sensors are also used to calculate the temperature of the surrounding area. The surrounding area that is too hot will result in a high humidity level. This will affect the time taken by the WIG model to take off. Relatively moist air flow will increase the friction with the hull WIG model. Figure 12 shows the installed telemetry system in the craft.

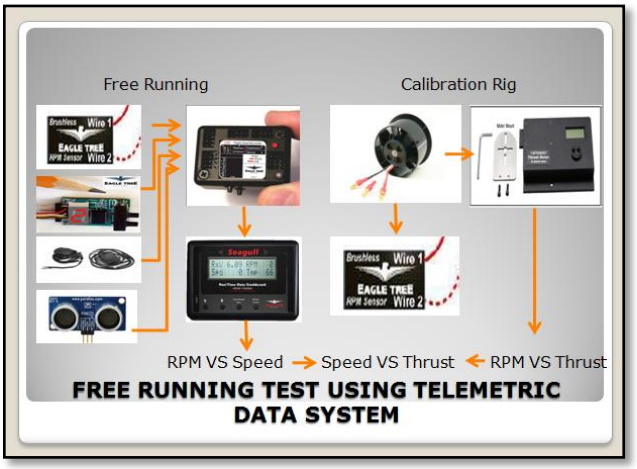


**Figure 12** Free running test schematic

## 4.0 RESULTS AND DISCUSSION

### 4.1 Aerodynamic Drag of Rectangular Wing

In this paper, the wing lift coefficients were numerically calculated using the vortex lattice method (VLM) and compared with the CFD calculation using FLUENT v6.0 and the published experimental results (Jung et.al [15]) for section NACA6409. The aerodynamic characteristics of the wind tests were performed at wind speed, 25.5 m/s (Rn = $3.49 \times 10^5$). The test results obtained agreed very well with each other. Figures 13 to 16 show that the lift coefficient varied with the angle of attack (AOA) as a function of the ground clearance for wings with two different aspect ratios (AR). The magnitude of lift coefficient increases with increment of aspect ratio (AR) and angle of attack (AOA), and low ground clearance (h/c), where c is the mean aerodynamic chord. According to Figures 13 to 14 lift coefficients of VLM and CFD results were close to published experimental results. It is known from these investigations that the lift coefficient is greatly increased with a decrease in the height above the surface *h/c*. It also pointed out that the aspect ratio of the wing has a strong influence on the lift at small separation distances from the surface, $h/c \leq 0.3$. Most of the existing designs of WIG crafts are not optimal from the viewpoint of surface aero-hydrodynamics, but after skillful overall arrangement, optimal configuration with high aerodynamic performance may be obtained.

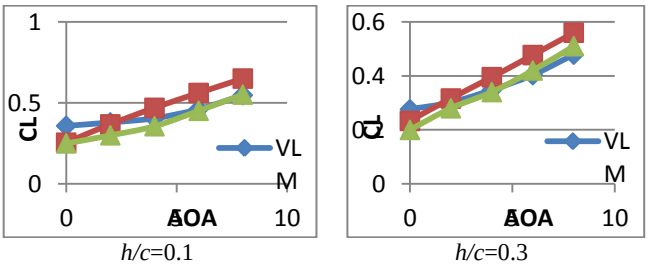


*h/c*=0.1 *h/c*=0.3

**Figure 13** Lift Coefficient versus AOA of rectangular wing *AR*=1

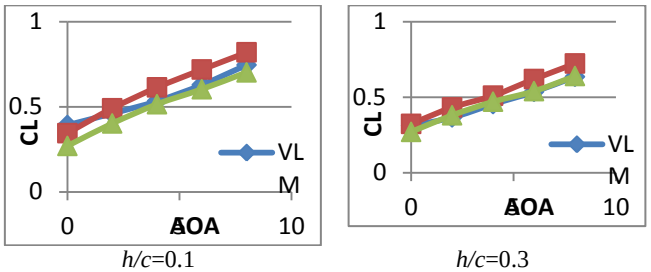


**Figure 14** Lift Coefficient versus AOA of rectangular wing *AR*=1.5

The drag coefficient varied with angle of attack for two aspect ratios (AR = 1 and 1.5) and two ground clearances (h/c = 0.1 and 0.3). In Figures 15 to16, the aspect ratio of the wing has no influence on the drag at small separation distances from the surface. However, it shows that the drag force of the wings with section NACA6409 at wind speed 25.5m/s was decreased by the ground effect as the wing approaches the ground. The reason for this may be that the induced drag decreases due to the reduction of the tip vortex at the wing tip. Because of the increase in lift and the decrease in drag at low ground clearance, the lift-to-drag ratio (L/D) increases due to the ground effect.

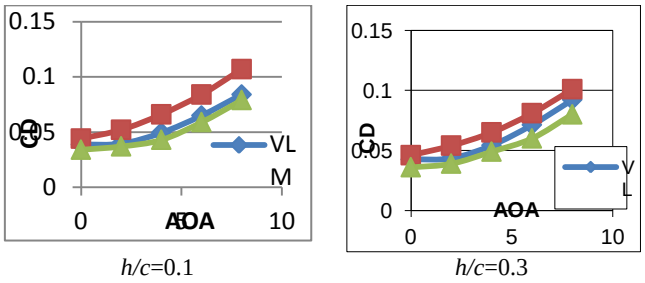


**Figure 15** Drag Coefficient versus AOA of rectangular wing *AR*=1

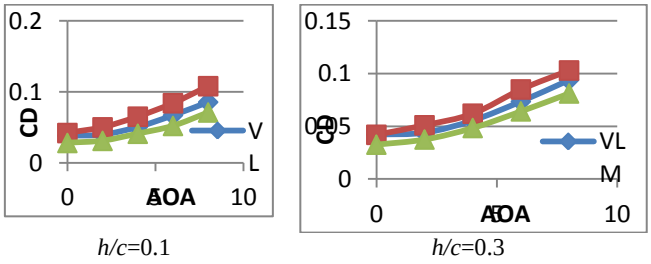


**Figure 16** Drag Coefficient versus AOA of rectangular wing *AR*=1.5

## 4.2. Aerodynamic Drag of Compound Dihedral Wing

The lift to drag ratio of rectangular and compound wings versus angle of attack at ground clearance (h/c) of 0.15 and aspect ratio 1.25 are plotted in Figure 17. The increment of lift to drag ratio of compound wing compared to rectangular wing and it was found that the increment of lift to drag ratio of compound wings is valuable especially for compound wing (C-4) because of the higher lift. Compound wing-1 (C-1) has middle span of 50%, compound wing-2 (C-2) has 45% middle span, compound wing-3 (C-3) has 40% middle span and compound wing-4 (C-4) has 30% middle span from total wing span. Therefore compound wing-4 (C-4) had smaller middle span and larger dihedral side span compared to others. The variation of this increment at any angle of attack was high. The maximum increment occurred at the angle of attack 4° for each compound wing where for compound wing-4 (C-4) it was around 20%. This increment can be related to the high efficiency, energy-saving and the reduced environmental impact of present compound wing.

The lift to drag ratio of compound wing-4 (C-4) versus anhedral angle is summarized in Figure 18. The increment of lift to drag ratio of compound wings is valuable especially at large anhedral angle. For example, the increments were 17.6 and 25.7 percent at anhedral angles of $13^0$ and $15^0$ respectively. This increment can be related to the high efficiency, energy-saving and the reduced environmental impact of the present compound wing. The trend of lift to drag ratio versus anhedral angle of compound wings has a sharp increase with the rise of anhedral angle which means that the variation of lift to drag ratio was high.

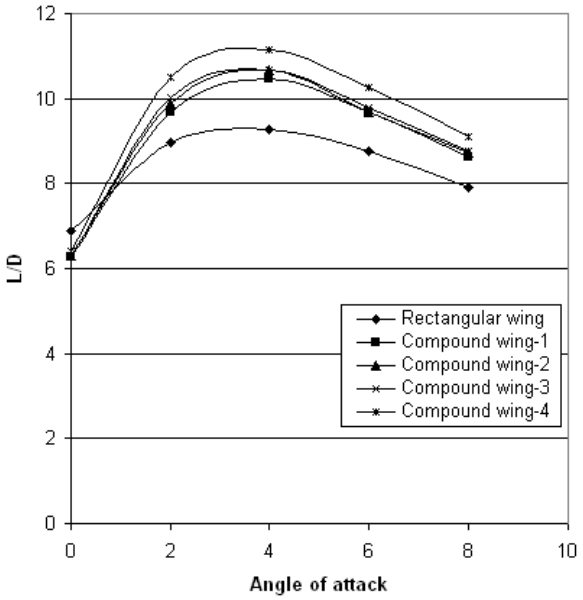


**Figure 17** The lift to drag ratio versus AOA of rectangular and compound wings

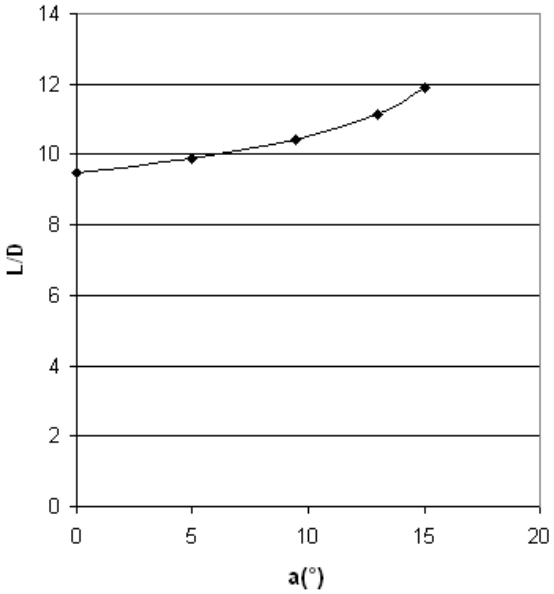


**Figure 18** The lift to drag ratio versus anhedral angle ($a^0$) of compound wing-4 (C-4)

### 4.3 Fight Tests Model

The surface effect aero-hydrodynamics is mainly concerned with various complex phenomena and characteristics of bodies moving closely near air-water surface [16]. It was discovered in the early part of this century that such a surface has a great influence on the aerodynamic characteristics of a vehicle flying close to it. An increase in lift is experienced during flight. Comprehensive reviews on the development of surface aero-hydrodynamics and the design philosophies of the surface craft are given by Rozhdestvensky [17] and Cui [16].

The WIG configuration is usually complex, with wing, fuselage, tail planes, end-plates and control surfaces, and so calculation of the aero-hydrodynamics is very complicated. Hence, analysis and design have to rely mainly on experimental data.

Flight test were conducted by gradually incrementing the thrust motor. The take off distance and airspeed were then evaluated. Several videos were taken and it was evident that the craft has achieved Ground Effect (GE), with the evidence of an air gap just below the craft (Refer to Figures 19 to 22). Fluctuation of thrust has been generated and this has enabled the craft to sometimes lift off the water surface initially before stabilizing in forward motion. The craft is attempting to enter into ground surface effect at design speed of 10.28 m/s. The most significant observation regarding propulsion during most of the flight tests has been occasional stalls and flips. The stern portion has been observed to be heavy.

The thrust was calculated for each RPM reading during flight test by refering to the calibration data. It has been determined that a minor flaw in design exists at the bottom of the outrigger hulls. The hull should be further leveled to the wing to achieve further reduction in excess weight and improving the lift underneath. Since the initial thrust of the model would have lifted the hull out of the water, by leveling it with the wing would mean that hydrodynamic drag on the hull is removed from start and the entire craft would have maximum lift due to the flat plate configuration. Testing has led to the craft flying in surface effect with an air gap (elevation) measured at the simple piece of rope (attached to the bottom of the craft) up to 0.05m in between the hull and water surface.

**Figure 19** Start to take off

**Figure 20** Take off with Elevation 0.03m

**Figure 21** Take off with Elevation 0.04m

**Figure 22** Take off with Elevation 0.05m

The batteries were prepared at different distances, starting from forward part of WIG model. The actual centre of gravity (LCG) for this model was 0.06 m from forward part and would be varied, it based on the position of battery. But the maximum and minimum LCG were still kept in the range to enable the WIG model to take off. By moving the batteries aft ward, the centre of gravity (LCG) for WIG model would be shifted. Two batteries were used in the flight test. For different distance of battery from forward perpendicular, it would give the movement of LCG and affected the elevation. Each elevation would also affect the lift coefficient (CL), as observed. It was also shown that the calculated results are satisfactory even at close proximity to ground surface ( $h/c \leq 0.2$ ).

## ■5.0 CONCLUSION

The conclusion of the study of the estimation of propulsive power required for Wing in Ground effect (WIG) craft to take off; can be drawn as follows;

(1) Savitsky's method and Vortex Lattice Method which were used to calculate the surface effect of aero-hydrodynamic for water drag and aerodynamic drag, respectively, are in good agreement with the measured experimental one.
(2) The required propulsive power for craft scaled model was calculated at the design air speed of 10.28m/s to give the total thrusts of 33.85 N, it used the configuration of two propellers each of which was 17 N. The effective power estimates required for WIG model to take-off per propeller based on Froude's momentum theory was 128Watt at the design speed.
(3) Flight tests results show that the craft is attempting to enter into ground surface effect at design speed and the most significant observation regarding propulsion during most of the flight tests has been occasional stalls and flips.

### Nomenclature

| | |
|---|---|
| $AR$ | Aspect Ratio ( b/c ) |
| $b$ | Wing Span ( m ) |
| $c$ | Chord length ( m ) |
| $C_M$ | Moment Coefficient (=L/0.5ρAU$^2_\infty$ ) |
| $C_L$ | Lift Coefficient (=L/0.5ρAU$^2_\infty$ ) |
| $C_D$ | Drag Coefficient (=D/0.5ρAU$^2_\infty$ ) |
| $C_{Di}$ | Induced Drag Coefficient |
| $h/c$ | Ground clearance |
| $N$ | Maximum number of element panel |
| $c_c$ | cord along trailing leg of elemental panel (m) |
| $\alpha$ | Angle of attack ( $^0$ ) |
| $\phi$ | Dihedral angle ( $^0$ ) |
| $\sigma$ | Ground Influence coefficient |
| $\psi$ | sweep Angle ( $^0$ ) |
| $\rho$ | |
| $\Gamma$ | |
| $F$ | |

| | |
|---|---|
| $S$ | air density |
| $U$ | vortex strength |
| $u$ | |
| $v$ | Influence function geometry of single horshoe wing area ($m^2$) |
| $w$ | free stream velocity (m/s) |
| | backwash velocity (m/s) |
| | sidewash velocity (m/s) |
| | downwash velocity (m/s) |
| $r_1$ , $r_2$ | vector distance |
| $\bar{x}, \bar{y}, \bar{z}$ | body axis system for plan form |
| $\hat{x}, \hat{y}, \hat{z}$ | wind axis system |
| $X,Y,Z$ | Axis system for horshoe vortex |
| $X_{ac}$ | distance center of aerodynamic from leading edge |
| $X_{cg}$ | distance center of gravity from leading edge |
| $X_h$ | distance center of height from leading edge |

## Acknowledgement

The authors would like to thank Universiti Teknologi Malaysia (UTM) and Ministry of Science, Technology and Innovations of Malaysia (MOSTI) for the financial support towards conducting the study. The authors also express their earnest gratitude to head and staffs of Research Management Centre (RMC), UTM for the administrative management during the study.

## References

[1] Nikolai, K and Konstantin, M. 2003. Complex Numerical Modelling of Dynamics and Crashes of Wing-In-Ground Vehicles, AIAA Papers, AIAA 2003-600. American Institute of Aeronautics and Astronautics.
[2] Ghassemi, H., Ghiasi, M. 2008. A Combined Method for the Hydrodynamic Characteristics of Planing Crafts. *Ocean Engineering*. 35: 310–322.
[3] Lai, C. and Troesch, A. W. 1996. A Vortex Lattice Method for high Speed Planing. *International Journal of Numerical Method in Fluids*. 22: 495–513.
[4] Zhao, R., Faltinsen, O. M and Haslum, H. A. 1997. A Simplified Nonlinear Analysis of a High Speed Planing Hull in Calm Water. Proceedings 4th Int. Conf. on Fast Sea Transportation, Australia.
[5] Savander, B. R., Scorpio, S. M., Taylor, R. K. 2002. Steady Hydrodynamic of Planing Surface. *J. of Ship Research*. 46(4): 248–279.
[6] Xie, Nan, Vassalos, Dracos, Jasionowski, Andrzej. 2005. A Study of Hydrodynamics of Three-dimensional Planing Surface. *J. of Ocean Engineering*. 32: 1539–1555.
[7] Wang, D.P., Rispin, P. 1971. Three-dimensional Planing At High Froude Number. *Journal of Ship Research*. 15 (3): 221–230.
[8] Cheng, X., and Wellicome, J.F. 1994. Study of Planing Hydrodynamics Using Strips of Transversely Variable Pressure. *J. of Ship Research*. 38: ( 2): 30–41.
[9] Clement, E. P and Blount. 1963. D. L. Resistance Tests of Systematic Series of Planing Hull Forms, SNAME Transaction. 71: 491–579.
[10] Katayama, Toru, Hayashita Shigeru, Suzuki Kouji and Ikeda Yoshiho. 2002. Development of Resistance Test for High-Speed Planing Hull Using Very Small Model-scale Effects on Resistance Force-Proceedings of Asia Pacific workshop on Hydrodynamics.7–14.
[11] Savitsky, D. 1964. Hydrodynamic Design of Planing Hulls. *Marine Technology*. 1(1): 71–95.
[12] Steinbach, D, and Jacob, K. 1991. Some Aerodynamic Aspect of Wings Near Ground. *Trans. Jpn. Soc. Aeronaut. Space Sci*. 34: 56–70.
[13] International Towing Tank Conference. 1957. Chapter VII Model Resistance Test Techniques, Madrid, Spain, ITTC 1957.
[14] Houghton, E. L. and Carpenter, P. W. 1993. *Aerodynamics for Engineering Students*. New York: John Wiley & Sons, Inc.
[15] Jung, H. H, Chun and Chang, C. H. 2002. Longitudinal Stability and Dynamic Motions of a Small Passenger WIG Craf. Elsevier. *Journal of Ocean Engineering*. 29: 1145–1162.
[16] Chui, E. 1998. Surface Effect Aero-Hydrodynamics and Its Applications. *Indian Academy of Sciences*. 23(5): 569–577.
[17] Rozhdestvensky, K. V. 1995. An Effective Mathematical Model of the Flow Past Ekranoplan with Small Endplate Tip Clearance in Extreme Ground Effect. Proc. Workshop on Twenty-First Century Flying Ship. 155–177.